

Old stellar population studies in multifilter spectro-photometric data

L.A. Díaz-García¹, A.J. Cenarro¹, and the ALHAMBRA Team*

¹ Centro de Estudios de Física del Cosmos de Aragón (CEFCA), Plaza San Juan, 1, Planta-2, E-44001, Teruel, Spain

Abstract

We present first results on the stellar population analysis for two samples of Early-Type galaxies (ETGs) up to $z \sim 1$ in the Advanced, Large, Homogeneous Area, Medium-Band Redshift Astronomical (ALHAMBRA) survey, allowing us to face how and when these galaxies were formed and have evolved throughout cosmic time. The analysis has been performed making use of a generic code developed by our team to study and recover the main parameters of old stellar populations as seen by large scale multi-filter surveys, such as J-PAS, J-PLUS or ALHAMBRA. The code is based in spectral energy distribution fitting techniques based on error-weighted χ^2 minimization tests and MonteCarlo (MC) simulations. We overall find that the bulk of the stellar content of ETGs was formed at high redshifts, showing hints for more massive ellipticals being 1 Gyr older than less massive ones.

1 Introduction

The narrow/broad-band multifilter surveys are placed halfway in between the traditional imaging and spectroscopic surveys. They make possible the study of many different astronomical problems in a self-contained way. These kind of surveys open a new possibility to study the stellar content of high- z galaxies through the comparison with multi-wavelength spectral energy distributions (SEDs) models. Template fitting makes possible that we can measure stellar population parameters, as photo-redshifts or stellar masses, at higher- z than the spectroscopy allowing us to explore new topics as the size effects of ETGs through the study of their stellar content, and their evolution along the cosmic time.

* <http://alhambra.iaa.es:8080/raquel/?q=content/alhambra-team>

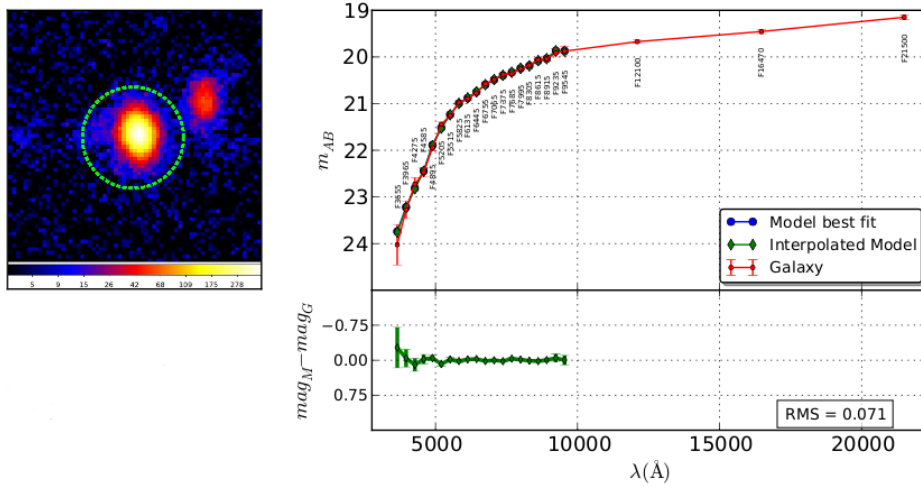


Figure 1: Spectral fitting of an ETG from ALHAMBRA using the MIUSCAT SSP SEDs. The photometry of the galaxy is plotted in red. The best MIUSCAT SSP fit (Age = 2.3 ± 1.3 Gyr; $[Z/H] = -0.4 \pm 0.4$ dex) to the galaxy photospectrum, as derived from a standard χ^2 minimization technique, is plotted in green. The residuals are shown in the lower panel with the same scale. On the left, the stamp of the galaxy is presented.

2 Data

Our data consists on a sample of ETGs of the ALHAMBRA V3 photometric catalogs. The ALHAMBRA survey provides a photometric dataset over 20 contiguous, medium-band, FWHM = 310 Å, top-hat filters, that cover the complete optical range from 3500 to 9700 Å over a total area of 4 deg² (low extinction) on the sky (see [13]), reaching $m_{AB} \sim 25$ (S/N=5, point-like source) for the sixteen bluer filters, and $m_{AB} \sim 23.5$ for the four reddest filters. The optical coverage is supplemented with the standard NIR J , H , K_s filters which have a 50% detection efficiency depth of $J \sim 22.4$, $H \sim 21.3$, and $K_s \sim 20.0$ (see [8]). To build our sample, we use the photo-spectral classification developed in [14] for this survey, based in the Bayesian Photometric Redshift estimation (BPZ, see [1]). To produce quality results, we just select the ETGs that have a mean signal to noise ratio larger than fifteen with eleven ALHAMBRA filters available or more. Our sample contains 5395 ETGs with these constrains.

3 Analysis techniques

To determine the stellar parameters of old stellar populations, we have developed a generic code focused on large scale multifilter surveys, such as ALHAMBRA (see [13]), J-PLUS (see [5, 6]) or J-PAS (see [2, 5]).

The analysis techniques are based in an error-weighted χ^2 minimization test to match the multi-wavelength SEDs of a model set, convolved with the survey filters, with the galaxy

photospectra. The program carries out a MC method, using the proper signal to noise of each filter, to estimate the errors in the parameters of the stellar populations. As output, the code recovers the redshift of the galaxy, the dust extinction, the initial Mass function (IMF) slope, the stellar mass, the luminosity weighted age and metallicity and their errors. So far, emission lines are detected and masked out for the SED fitting. To increase the accuracy of the galaxy parameters, biased by the parameter coverage of the proper model SEDs, the code interpolates (not extrapolates) the SED templates around the best solution to get new models with more precise metallicities, ages and extinctions. The analysis technique details will be presented in [9].

The basic input of the code is composed by three components: the first component is a spectral library of single stellar populations (SSPs); the second component is the photometric system with the transmissions curves of the filters to convolve with the models; and the last component is the photometry of the galaxies with errors. Before the convolution stage, we extend the spectral library of models for different redshifts and extinction values to get more realistic spectra. As extinction laws to apply over the SSPs, we use the parametrized extinction in [3]. We assume that, statistically, the main factor of extinction is dust, consequently, we adopt $R_V = 3.1[\equiv A_V/E(B - V)]$ for this extinction parameter (indicator of environmental characteristics).

To illustrate, in Fig. 1 we can see the best SED fitting derived for the photospectrum of an ALHAMBRA ETG, using the MIUSCAT SSP models (see [19, 15]) as input templates. MIUSCAT SSP models have been convolved with the ALHAMBRA filters to simulate a real case. It is clear from the figure that the best fitting, derived from a our χ^2 minimization technique, reproduces well the observed spectrum at both low and high frequencies. The obtained residuals are shown in the lower panel. The best solution corresponds to a MIUSCAT SSP model of 2.3 ± 1.3 Gyr and metallicity (-0.4 ± 0.4 dex).

4 Results

We present first results on the stellar population analysis employing our tool fitting. We use as input the MIUSCAT V9.2 SSP templates with a preliminary ultraviolet extension (from 1860\AA to 3500\AA) of the models (see [20]) which were convolved with ALHAMBRA filters.

4.1 Photo-redshifts

To prove that our code retrieves adequate photoredsifts for old stellar populations in multifilter surveys, we check the accuracy of our photoredsifts over a subsample of ALHAMBRA ETGs in common with the spectroscopic database of zCOSMOS 10k-bright (see [12]). To get a reliable subsample of ETGs we use the morphological classification in [16] of the COSMOS galaxies.

As result, the Fig. 2 shows the comparison, one by one, between our redshifts and the high quality spectroscopic redshifts of the sample. We check that there exists a very good agreement between the photometric and spectroscopic redshifts, and the redshift error

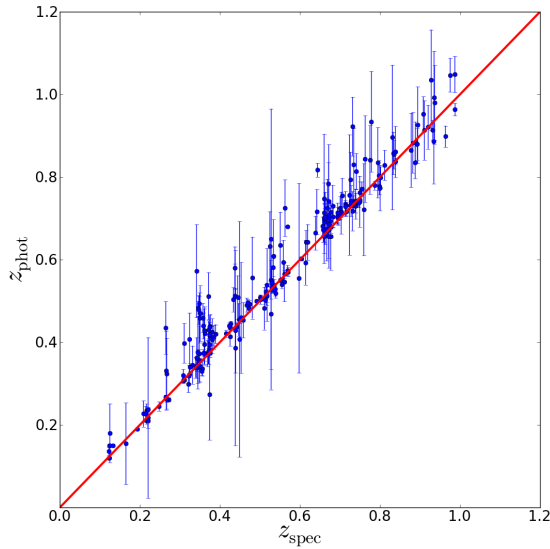


Figure 2: Photometric redshifts of the ETG sample. We compare the photometric redshifts (y-axis), obtained with our techniques, with the spectroscopic redshifts (x-axis) from zCOSMOS 10k-bright. The red line represents the 1:1 relation. Considering the errors, for a confidence level of 1σ , we get photoredsifts in perfect agreement with spectroscopic redshifts.

estimations of our method are reliable (Fig. 2). These first results show that the analysis techniques, together with the MC process to estimate the errors, provide compatible results with spectroscopic measurements.

4.2 Stellar populations

We present the results on the stellar population analysis allowing us to face how and when these galaxies were formed and have evolved throughout cosmic time. In addition, we have tested the well-known relations between metallicity–stellar mass, age–metallicity and age–stellar mass, using our analysis techniques on the ALHAMBRA ETG sample, to check that the code is getting consistent results with previous works.

Regarding Fig. 3, both average metallicity and age increase along the sequence of ETGs with stellar masses in $10^9 - 10^{12}M_{\odot}$. The above results indicate that young and metal-poor stellar populations are found predominantly in lower mass ETGs according with previous works (e. g., [11, 18]). This would imply that the low stellar mass galaxies appear metal-poor because they have not had time to produce metals by star formation, contrarily, the more massive ETGs present high metallicities due to they had more time to produce heavier elements. This is consistent with a 'downsizing' scenario, in which the mass and luminosity of the galaxies become progressively lower as the Universe becomes older (see [7]).

We have study the formation epochs of ETGs exploring the typical age of the stellar populations as a function of their masses along the cosmic time. We splitted the sample in

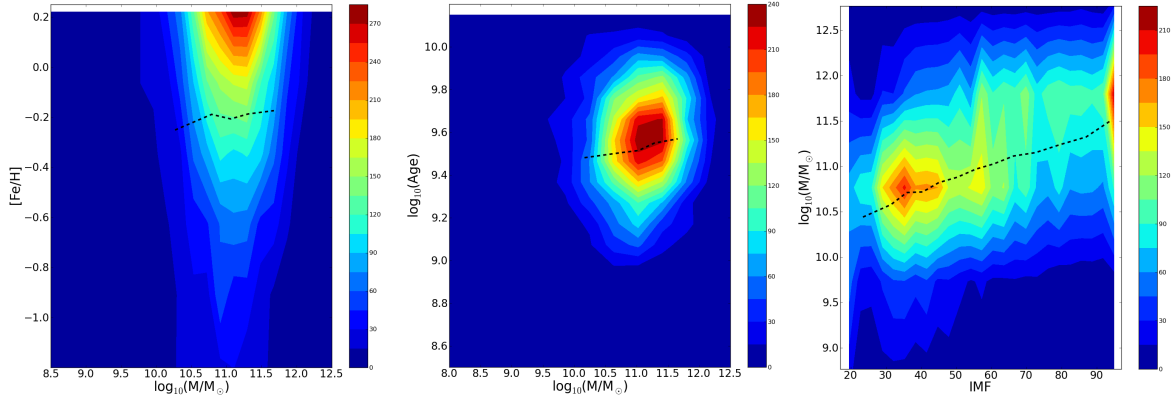


Figure 3: Density surfaces of the parameters obtained. A redder (bluer) color in the density surfaces indicates a higher (lower) density of galaxies with the physical parameters. The color bars indicate the value ranges of the density surfaces. The discontinuous black lines are the averages of the parameters. *Left panel:* shows the density surface of the stellar mass (x -axis) versus metallicity (y -axis). *Centre panel:* density surfaces of stellar mass (x -axis) versus age (y -axis). *Right panel:* density surfaces of IMF slope (x -axis) versus stellar mass (y -axis). The above results indicate that young, metal-poor stellar populations are found predominantly in lower mass ETGs in accordance with a downsizing scenario. We can see that the massive galaxies are better fitted with a bottom heavy IMF where there exists an excess of low mass stars. Similar results had been found in previous works using spectroscopy.

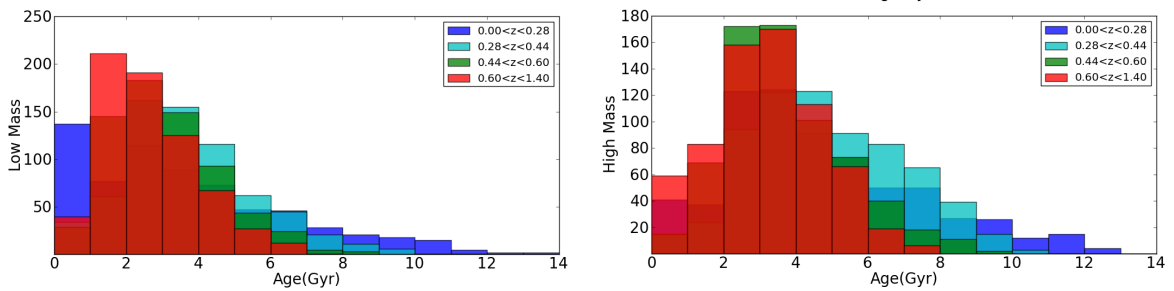


Figure 4: Age histograms of ETG sample at different redshifts for the case of low stellar mass (left panel) and high stellar mass (right panel). Massive ellipticals are ~ 1 Gyr older than the lower mass ETGs at the same cosmic time which confirm that the more massive galaxies were formed in an earlier epoch.

four redshift bins and every redshift bin is splitted in two stellar mass bins separating the more massive galaxies and the low mass galaxies for every epoch. We have ~ 650 galaxies in every bin to analyse the average age of the galaxies. On the left of the Fig. 4 we can see the age histograms for different cosmic times for low stellar mass ETGs and on the right for the massive galaxies. The Fig. 4 shows that the massive galaxies are ~ 1 Gyr older than the lower mass ETGs at the same cosmic time which confirm that the more massive galaxies were formed in an earlier epoch and suffered an episode of star formation more efficiently than the lower stellar mass, this result is in agreement with works as [17].

In Fig. 3 we plot the density surface of stellar mass versus IMF slope, we find a correlation between the slope of the IMF and the mass of the galaxy. We can see that the massive galaxies are better fitted with a bottom heavy IMF where there exists an excess of low mass stars respect giant stars. This necessity of an excess of low mass stars was found to explain some features in the spectra of massive galaxies in previous papers such as [4]. Recently [10] presents an observational evidence that low mass ETGs are better fitted by a bottom-light IMF with a Kroupa-like function, whereas massive galaxies require bottom-heavy IMFs, even exceeding the Salpeter slope.

References

- [1] Benítez, N. 2000, ApJ, 536, 571
- [2] Benítez, N. , Gaztañaga, E., Miquel, R., et al. 2009, ApJ, 691, 241
- [3] Cardelli, J. A., Clayton, G.C., & Mathis, J.S. 1989, ApJ, 345, 245
- [4] Cenarro A. J., Gorgas, J., Vazdekis, A., et al. 2003, MNRAS, 339, 12
- [5] Cenarro A. J., Moles M., Cristóbal-Hornillos D., et al. 2010, SPIE, 7738
- [6] Cenarro A. J., et al. 2012 in prep.
- [7] Cowie, L. L., Songaila, A., Hu, E. M., et al. 1996, AJ, 112, 839
- [8] Cristóbal-Hornillos, D., Aguerri, J. L. A., Moles, M., et al. 2009, ApJ, 696, 1554
- [9] Díaz-García, L. A., et al. 2012, in prep.
- [10] Ferreras, I., La Barbera, F., Carvalho, R. R., et al. 2012, arXiv:1206.1594F
- [11] Gallazzi, A., Charlot, S., Brinchmann, J., et al. 2005, MNRAS, 362, 41
- [12] Lilly, S.J., Le Brun, V., Maier, C., et al. 2009, ApJS, 184, 218
- [13] Moles, M., Benítez, N., Aguerri, J. L. A., et al. 2008, ApJ, 136, 1325
- [14] Molino, A., et al. 2012, in prep.
- [15] Ricciardelli, E., Vazdekis, A., Cenarro, A. J., et al. 2012, MNRAS, 424, 172
- [16] Tasca, L. A. M., Kneib, J. P., Iovino, A., et al. 2009, A& A, 503, 379
- [17] Thomas, D., Maraston, C., Bender, R., et al. 2004, arXiv:astro-ph/0410209
- [18] Tremonti, C. A., Heckman, T. M., Kauffmann, G., et al. 2004, ApJ, 613, 898
- [19] Vazdekis, A., Ricciardelli, E., Cenarro, A. J., et al. 2012, MNRAS, 424, 157
- [20] Vazdekis, A., et al. 2012, in prep.